Identifying Pitfalls in Lithium Metal Battery Characterization

Eric Winter,[a] Thomas J. Schmidt,[b, c] and Sigita Trabesinger*[a]

Over the past decade, there has been a revival of research activity on lithium metal batteries (LMBs) as these could be a solution for key challenges of electromobility and the energy revolution. While there is growing consensus in the scientific community that common reporting standards and testing conditions for LMBs have to be established, a vast majority of research activities on lithium metal use lab-dependant testing protocols. For that reason, this publication aims to shed light on various, potentially neglected aspects in battery assembly and testing. Firstly, the long-term cycling, regarding a range of experimental parameters, such as current density, capacity, electrolyte type and its quantity, as well as contribution of the electrode edges, is shown in both symmetric (Li||Li) and asymmetric (Cu||Li) configurations. The second part focuses on the reversibility of lithium thickness during cycling with and without protected electrode edges, investigated by operando dilatometry. By bringing the insights from this parameter study together, we aim to contribute to better experiment design for future LMB studies, as well as a better understanding for the failure mechanism of Li metal anodes.

1. Introduction

In an age characterized by a shift towards renewable energies and electromobility, there is an ever-increasing need for potent energy storage. Lithium-ion batteries (LIBs), a technology that has already found wide application in portable electronics, are set to be one of the most important energy storage options available in the future. To make them an economically even more viable, increasing their energy density would be highly desirable, which has led to focus in battery research on increasing the capacity and voltage window of LIBs by modifying either cathode or anode materials. Here, one of the most promising candidates for next-generation anodes is metallic lithium, which would not only remove the need for a graphite intercalation electrode, but also be highly attractive due to its high specific capacity ($3860 \ mAh \cdot g^{-1}$) and negative redox potential ($-3.04 \ V$ vs. SHE). Lithium metal was already subject to intensive research in the 1960s–1970s,[1–4] where immense efforts were made to come up with new means of energy storage for defence and space exploration.[5] Relatively early, however, the shortcomings of lithium metal, including the poor reversibility of batteries containing metallic Li, were discovered.[1,3,6] First attempts to make lithium-based secondary batteries included a combination of lithium with a TiS_2 electrode,[7–9] but the real breakthrough did not occur before the late 1980s, when graphite intercalation electrodes were first utilised.[10,11] Since then, graphite almost completely replaced metallic Li in commercial cells, and research on lithium metal batteries was, after decades of continued efforts, widely abandoned, as no viable solutions for common problems, such as dendrite formation and high reactivity towards most organic electrolytes had been found. With the new millennium and an increasing demand for high-energy batteries, the primary approach was therefore to work on new cathode materials rather than lithium anodes, which were long considered as "too dangerous".[12] Only recently, a drastic increase of new studies addressing the deficiencies of metallic lithium could be noticed.[13] Eventually, eliminating the graphite anode as a battery component would be desirable in several aspects. Not only would lithium metal increase the energy density as compared to typical lithium-ion batteries by a factor of 1.5–2[14] due to the decrease the anode's, and consequently the cell's, volume, making it even more appealing for energy storage in applications where both weight and space are major constraints.

Nevertheless, there are several issues in LMB research to be overcome in order to enable a breakthrough of this technology. Firstly, a rather small percentage of studies actually addresses the fundamental understanding of the detrimental processes in metallic lithium anodes. In addition, the effects of experimental parameters often are not taken into account, similarly to the Li–S case some years ago.[15,16] Top-down approaches elaborating remedies to certain aspects, e.g. dendrite formation and extended cycling-life, are much more prevalent[17–22] than bottom-up strategies where the aim is to develop a better

[a] E. Winter, Dr. S. Trabesinger
     Battery Electrodes and Cells, Electrochemistry Laboratory
     Paul Scherrer Institute
     Forschungsstrasse 111, 5232 Villigen PSI, Switzerland
     E-mail: sigita.trabesinger@psi.ch
[b] Prof. T. J. Schmidt
     Energy and Environment Division
     Paul Scherrer Institute
     Forschungsstrasse 111, 5232 Villigen PSI, Switzerland
[c] Prof. T. J. Schmidt
     Laboratory for Physical Chemistry
     ETH Zurich
     8093 Zurich, Switzerland

Batteries & Supercaps

Articles
doi.org/10.1002/batt.202100145

Chemistry Europe
European Chemical
Societies Publishing

understanding of the mechanisms leading to (and parameters indicating) battery failure[23–26] and exclude the effects of the particular experimental set up and conditions.

The lack of uniformity concerning testing conditions is rather worrying. A strategy to improve the performance of LMBs might look very promising, yet a comparison to related studies might be difficult due to the disparity of boundary conditions between them. For example, a coating might work excellently at a current density of 0.5 mA·cm^{-2} or 1.0 mA·cm^{-2} in a certain system, but could be entirely useless when implemented in a different environment or exposed to harsher conditions. In relation to issues like that, there have recently been calls from the scientific community to move towards common, strict reporting standards to facilitate the exchange of ideas and thus boost LMB research.[27–29] A related aspect, which should also be critically evaluated, is the influence of the different battery components. Not understanding their impact on an experiment or even neglecting it altogether can only lead to a poor reproducibility of a measurement – while talking about it, reproducibility reporting in LMB studies is also an issue. In the worst case, such negligence has a potential to lead to wrong decisions when developing an improvement strategy for the stability of metallic lithium. Gaining a comprehensive understanding of the system one is working with is a key factor in accelerating sustainable solutions for the shortcomings of metallic lithium.

Therefore, our approach in this study is not to develop another remedy to fight the disadvantages of metallic lithium. Instead, we intend to shed light on influential factors and components in the cell assembly and characterization of LMBs. This requires a systematic study to quantify the influence of some known parameters, such as current density, amount and speed of lithium metal moved, and type and quantity of electrolyte. This will take place in the framework of long-term tests for an evaluation of cell stability and voltage profile. On the other hand, we want to better understand the processes occurring during lithium plating and stripping by *operando* dilatometry.

Based on these results, we will discuss why and how the potentially neglected parameters could have a significant impact on the outcome of measurements and in what way the findings in our work can be used to contribute to a more reliable baseline for future LMB tests. The ultimate goal is to make well-informed decisions when working on the utilization of lithium metal as a safe and viable anode material for the next generation of rechargeable batteries.

2. Results and Discussion

2.1. Symmetric Cells (Li||Li)

In the first part of this study, experiments were carried out with a series of symmetric (Li||Li) cells to obtain a comprehensive baseline and understand the influence of electrolyte amount in the cell, current density applied, and amount of cycled lithium on the lifetime and polarization induced in each of two

electrolyte formulations. The first electrolyte, in the following referred to as 'carbonate' electrolyte, is a mixture of fluoro-ethylene carbonate (FEC) and dimethyl carbonate (DMC) (v:v = 1:1) with 1 M of LiPF$_6$ salt, known to be effective for the suppression of dendritic growth and short circuits.[30] The second electrolyte, in the following simplified to 'ether' electro-lyte, is a mixture of 1,2-dimethoxyethane (DME) and 1,3-dioxolane (DOL) with 1 M lithium bis(trifluoromethanesulfonyl) imide (LiTFSI), as is typically used in lithium-sulfur cells, which function well for long-term cycling.[16] For exact composition of these two electrolytes including mixing ratios and salts used, please refer to the experimental section.

2.1.1. Influence of Current Density

The cycling rate of a cell – with the current density being the equivalent quantity in the context of symmetric cells – is a factor that typically has a crucial impact on the lifespan of a cell.[31–36] The behaviour of metallic lithium at different current densities has already been investigated versus common cathode materials,[35] however, we decided to first focus on a systematic experiments in symmetric configuration, since it is the typical model system for developing improvement strat-egies. Studying the influence of current density on the battery lifetime and overpotentials was therefore an intuitive starting point. We were looking at the impact not only of the applied current density, but also of the amount of lithium metal moved between the two electrodes in a cycle. In a first set of experiments (Figure 1), we were cycling the cells at current densities between 0.1 mA·cm^{-2} to 2.0 mA·cm^{-2}, with a step time of one hour, resulting in a cycled metal layer thickness between 0.5 μm and 10 μm. Corresponding voltage profiles of selected cycles can be found in Figure S1. In a second set-up (Figure S2), the cycled Li-metal amount, corresponded to the thickness of 10 μm, where the cells with high current densities had shorter charge and discharge times (Figure S2d, 1 h at 2 mA·cm^{-2}), and the ones running at lower current densities – longer half-cycles (Figure S2a, 20 h at 0.1 mA·cm^{-2}).

In general, the expected trends[37] for increasing instability and degradation with increased current densities were con-firmed. As can be seen in Figure 1, the higher the applied current density is, the higher the resulting overpotentials are for both carbonate and ether electrolyte-filled cells, it being more severe the carbonate.

However, when looking at results of the highest current density used (Figure 1d), a drastic divergence between the cycling performance in carbonate and ether electrolytes can be observed, with the carbonate electrolyte resulting in average polarization of up to 130 mV. Compared to that – while a voltage increase with rising current density can also be seen for the ether electrolyte-filled cells – the average polarization here does not exceed 50 mV, even at the highest current density used. Yet, with high current densities, a tendency towards sporadic voltage increases and spikes emerge (Figures 1 and S1). Contrary to expectations, these elevated voltages disappear after a couple of cycles and do not lead to irreversible cell
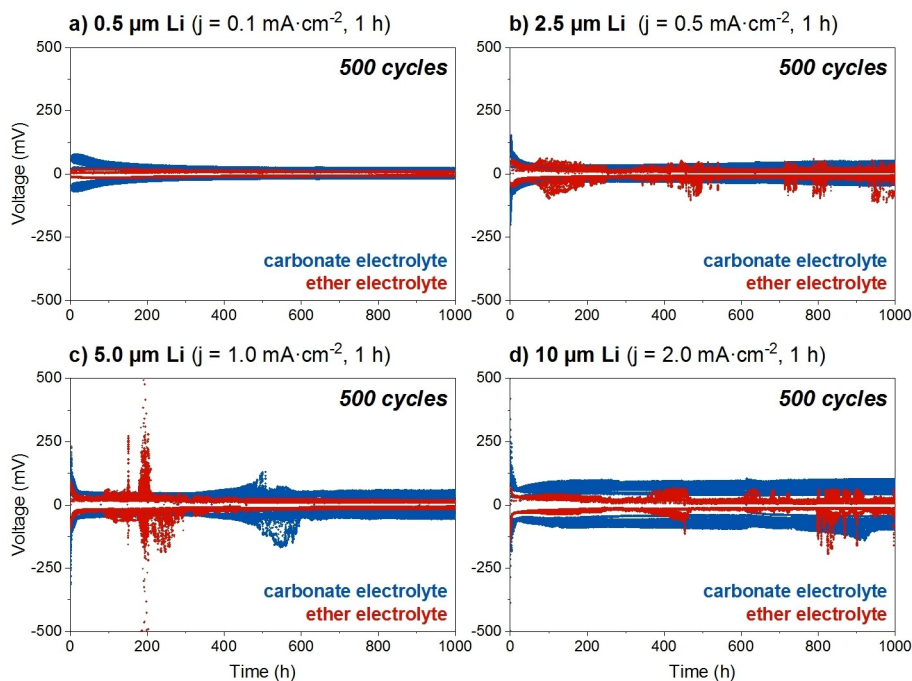
Batteries & Supercaps

Articles
doi.org/10.1002/batt.202100145

**Chemistry
Europe**
European Chemical
Societies Publishing

Figure 1. Polarization development of symmetric (Li∣∣Li) cells cycled at different current densities.

failure, as would be expected if persistent dendrites had formed. Generally, while cycling efficiency cannot be determined for symmetric cells, it appears that, in principle, all cells survived for the entire testing period of 1000 hours. However, their true degradation degree cannot be objectively assessed, as the vast excess of lithium metal and electrolyte cover up degradation effects in LMBs.[38]

In a second experimental configuration, where the same amount of metal (corresponding to layer thickness of 10 μm) was transferred at various current densities and corresponding step times, different observations can be made. Figures S2 and S3 show the impact of the modified cycling protocol (instead of a fixed time, here we fix the amount of lithium transferred) on the behaviour of the cells. In the case of the carbonate electrolyte, an increased overpotential (as compared to the ether electrolyte) can be observed, especially at current densities of 0.5 and 1.0 mA·cm^{-2} (Figure S2b and c). At the same time, the stability of the cells does not seem to deteriorate, even though a much larger amount of lithium is moved per cycle. The only deviation from the otherwise uniform behaviour can be noticed after about 600 h for the measurement at 1.0 mA·cm^{-2}, where the cell voltage collapses temporarily, while with the ether electrolyte, the overall behaviour is similar to the first set of experiments seen in Figure 1, though with improved stability.

Observations from these two experimental setups indicate that cell stability is not solely influenced by the cycling rate/ current density. Instead, the current density and step time, that is, the number of cycles over the duration of the experiment, has an even higher impact on the cell stability than the applied current density alone.[34,39,40] This agrees well with the idea that most detrimental effects occur at the beginning or the end of a cycle: due to the onset of lithium nucleation (initiation of Li plating on one side) and the exposure of uncycled metal (especially at the end of Li stripping, on the other side), the electrochemical conditions are most favourable for side reactions. Higher overpotentials can in general be detected for cells with the carbonate electrolyte, when these are accompanied by pronounced U-shaped voltage profiles (Figure S4), indicating a tendency towards the nucleation of dendrites.[41,42] It is important to note, however, that this assumed formation of dendritic lithium does not necessarily lead to cell failure in the symmetrical cell configuration. This becomes especially visible in the second experimental configuration with always-identical amounts of metal cycled – the overpotential for the carbonate electrolyte is significantly increased, but at the same time, cells exhibit a very stable behaviour throughout the experiment. Finally, an important message is that despite the instabilities, a complete cell failure does not necessarily occur. This points at the concept of so-called "soft short-circuits",[43] where a conductive dendritic pathway is formed in a cell and a collapse of the overpotential can be observed instead of cell failure. Over prolonged cycling, these pathways may eventually be eliminated again, as the locally increased current is also leading to elevated temperature, and this allows the dendrite to dissipate back into electrolyte. Consequently, the cell recovers and continues to cycle normally.

2.1.2. Influence of Electrolyte Volume

The volume of an electrolyte used for cycling can have a crucial impact on the results of the experiment.[44] If too little electrolyte is present, a cell might perform very poorly or not at all as

Batteries & Supercaps

Articles
doi.org/10.1002/batt.202100145

**Chemistry
Europe**
European Chemical
Societies Publishing

the entire electrolyte repository is used up after only a few cycles due to side reactions. In the opposite case, if too much electrolyte is present, the performance might be artificially enhanced, as side reactions are obliterated by the vast excess of electrolyte present.[27] Consequently, the real picture of cell behaviour is covered up, leading to incorrect conclusions about performance. This becomes especially important when recalling that, for credible results and optimum energy density of the cell, a lean electrolyte compatible with lithium metal should be used, when working on a strategy to improve cell performance.[45] The goal of the next set of experiments, therefore, was to quantify the sensitivity of symmetric cells towards a reduced electrolyte volume by systematically lowering the quantity from the default 500 μL in increments down to 50 μL. All other conditions remained unchanged as in the first experiment; the same current densities ranging from 0.1 to 2.0 mA·cm^{-2} were employed. For reasons of clarity, only the lowest and the highest current density are shown in Figure 2, while the full set of data can be found in Figures S5–S8.

At a low current density of 0.1 mA·cm^{-2}, even drastically reduced electrolyte quantities do not seem to significantly affect the outcome of testing. The only clear difference that goes beyond usual variation can be seen for those cells tested with a lowest quantity (50 μL) of electrolyte, where overpotentials are slightly increased for both the ether and the

carbonate electrolyte, however, without any signatures of soft short-circuits or cell failure. Similar trends can be seen for a current density of 0.5 mA·cm^{-2} (Figures S5 and S7) and 1.0 mA·cm^{-2} (Figures S6 and S8), where highest overpotentials are seen always for the lowest electrolyte quantity, whereas for anything above 100 μL cell polarization is, apart from minor variation, rather similar.

At the highest current density tested (2.0 mA·cm^{-2}), differences become visible when comparing between the electrolyte volumes. The ether electrolyte generally exhibits lower overpotentials than the carbonate one; however, tendencies towards instabilities can be seen regardless of the electrolyte type (Figure 2). If a larger amount of electrolyte is present (250 and 500 μL), then soft short-circuits seem to dominate, as one can see from overpotentials temporarily going down to zero. The same principle still holds for the ether electrolyte at a reduced volume of 100 μL, however, in the carbonate electrolyte-filled cells, irreversible cell failures seem to be the case after about 750–800 hours of cycling. When going to even lower electrolyte volume (50 μL), steeply increasing cell polarization can be observed for both electrolytes after prolonged cycling. While for the carbonate, cells tend to fail after only 300–400 hours of cycling, overpotential spikes can be noticed throughout the full testing period for the ether, with no clear temporal dependency. Compared to that, at a current density
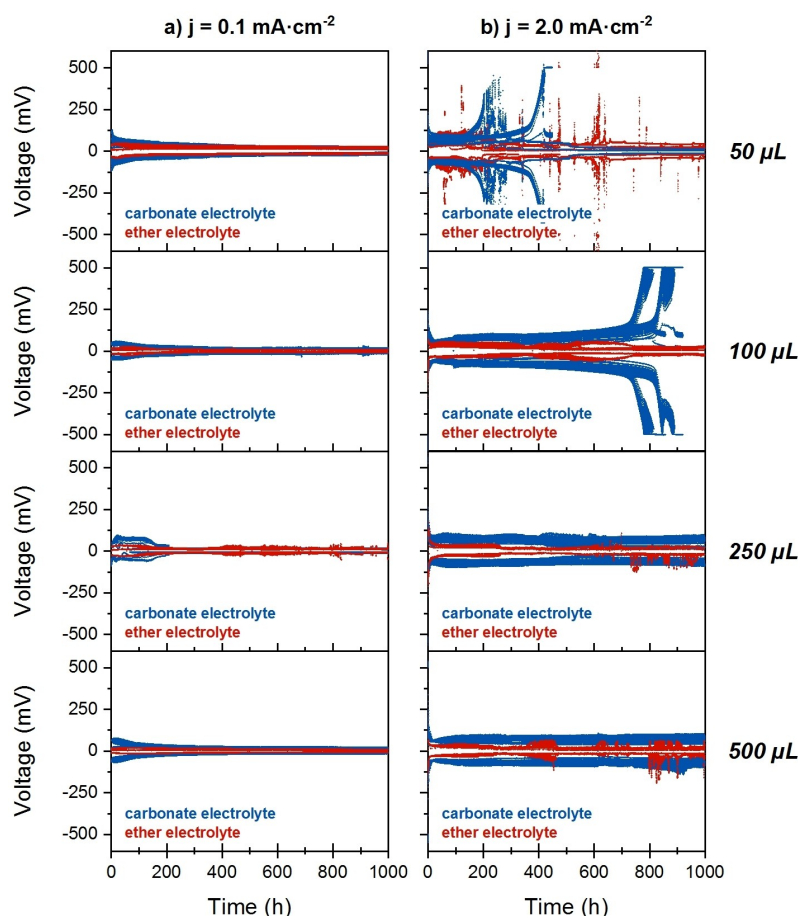

Figure 2. Polarization development at varied electrolyte volume. Only the lowest (0.1 mA·cm^{-2}) and highest (2.0 mA·cm^{-2}) current density tested are shown.

Batteries & Supercaps

Articles
doi.org/10.1002/batt.202100145

**Chemistry
Europe**

European Chemical
Societies Publishing

of 1.0 mA·cm^{-2} only the cells filled with the carbonate electrolyte start failing at the low electrolyte volumes, whereas the ether still allows – though at higher overpotentials – reasonably stable cycling down to 50 μL of electrolyte volume.

It can therefore be concluded that, in case of low to medium current densities (up to 1.0 mA·cm^{-2}), using a lean electrolyte (50 μL) is sufficient to obtain a realistic picture of cell behaviour. Using an excess of electrolyte does not contribute to higher cell stability or better performance. For the highest current density used in the tests, 2.0 mA·cm^{-2}, however, lean electrolyte conditions can only be applied up to a limited extent. Depending on the electrolyte, detrimental effects begin to show up at quantities of 100 μL and below, with polarization increasing steeply. This points to an increasing degradation of the electrolyte and unprotective SEI; eventually, the electrolyte is drying out completely, leading to high overpotentials and poor performance.[45] Therefore, a lean electrolyte in combination with high currents can be used for accelerated tests of potential remedies for lithium electrode instability. At the same time, the testing current should not strongly exceed the intended-use current ranges, as the good lithium solution can be missed, if too high currents are set. For that reason, with higher current densities (2.0 mA·cm^{-2} and possibly beyond), the objective of the experiment needs to be evaluated before choosing the right amount of electrolyte. If the main object of study is not electrolyte degradation and SEI formation, but for example, the general viability of an electrolyte or a certain lithium electrode design, slight excess conditions should be considered. In our case, volumes of 250 μL or more proved to be the best compromise between lowered electrolyte quantities and sufficient cell stability.

In either case, it is important to be aware of the consequences associated with the choice of electrolyte quantity as the failure mechanisms of a cell depends highly on the amount of electrolyte present. With a large excess of liquid, soft short-circuits dominate, which do not lead to complete cell failure but only temporarily reduce cycling overpotential, from which it can (but does not have to) fully recover. With a reduced electrolyte reservoir present, drying of the electrolyte is the much more prevalent mechanism, leading to irreversible cell failure.

2.2. Asymmetric Cells (Cu∥Li)

An identical testing matrix was applied to asymmetric Li-cells in order to understand the behaviour of lithium plating and stripping on a bare copper substrate, keeping in mind the desire for "anode-free" cells, where the only lithium reservoir is the cathode. The advantage of asymmetric cells is – while practically all experiments can be carried out in the same manner as with symmetric cells – that the efficiency of lithium metal cycling can be easily determined.[46] An advance study on the impact of copper substrate purity has been carried out (Supporting Information, Section C), concluding that pre-cleaned industrial-grade copper foils give similar results as the ones with high purity.

2.2.1. Influence of Current Density

Analogous to the Li∥Li experiments, the current density was varied by a fixed step time of 1 h in a first set of measurements (Figures 3 and 4), selected voltage profiles by cycle again shown in Figure S9. Again, in a second data set the step times were varied against a fixed amount (10 μm) of metal cycled (Figures S12 and S13). All experimental conditions were identical to those of symmetric cells. As can be seen in Figure 3, the
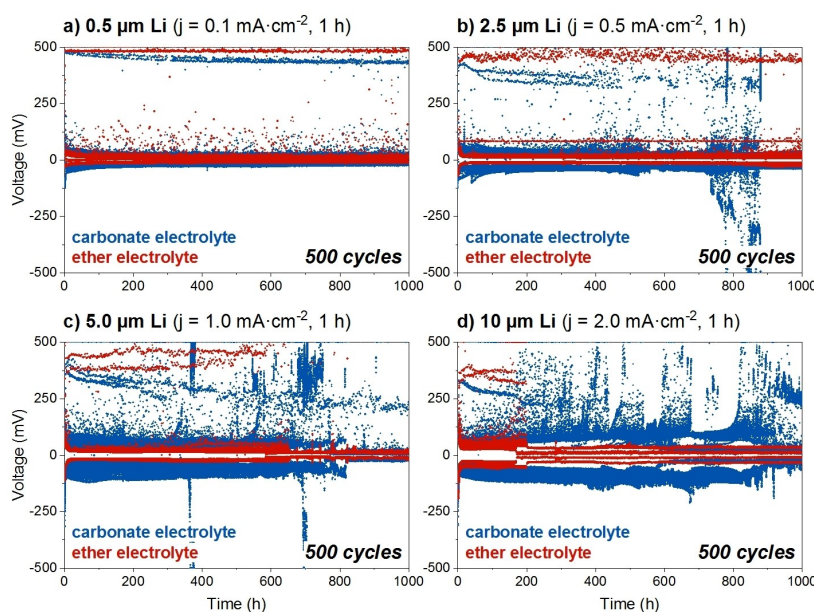

Figure 3. Polarization development of asymmetric (Cu∥Li) cells cycled at varied current densities and capacities.

Batteries & Supercaps

Articles
doi.org/10.1002/batt.202100145

Chemistry
Europe
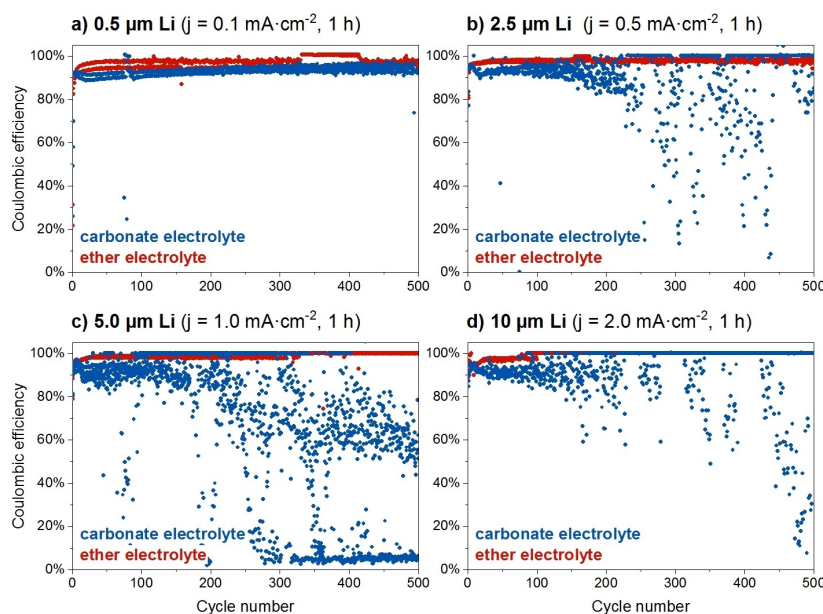European Chemical
Societies Publishing

Figure 4. Coulombic efficiencies of asymmetric (Cu||Li) cells cycled at varied current densities and capacities.

voltage profiles mostly resemble the ones seen for symmetrical cells (cf. Figure 1) for the first 100 hours. After that, differences start to arise, especially in the case of the carbonate electrolyte, where the effects of increased current densities are significantly more prominent than in symmetric cells.

At the two highest current densities (Figure 3c and d), cells with the carbonate electrolyte do not exhibit a similarly stable cycling behaviour as their symmetric counterparts (Figure 1c and d). In the case of the ether electrolyte, the differences to symmetric cells are not as drastic, with the exception of the cells tested at the highest current of $2.0 \, \mathrm{mA \cdot cm^{-2}}$. A main advantage of asymmetric cell tests compared to symmetric cells is that by looking at coulombic efficiencies (CE) it is possible to determine how efficient or inefficient lithium metal cycling actually is. This can be seen in Figure 4, where the true performance of the cells under the influence of different current densities is shown: cells, exposed to the lowest current density of $0.1 \, \mathrm{mA \cdot cm^{-2}}$ cycle relatively efficiently for the full duration of the experiment. In the case of the ether electrolyte, the CE plot also reveals some soft short circuits that occur after about 300 cycles (600 hours) and persist for a little less than 100 cycles, after which the cells surprisingly recover. The carbonate electrolyte also exhibits stable efficiency at the lowest current density, though slightly lower than the ether electrolyte. Looking at all the other current densities applied ($\geq 0.5 \, \mathrm{mA \cdot cm^{-2}}$), the short-lived stability of the carbonate cells, which was already seen in the copper substrate study (Figures S20 and S21), is again confirmed, with efficiency decreasing drastically and cells failing permanently after only about 100–200 cycles. Under the harsh conditions of a current density of $2.0 \, \mathrm{mA \cdot cm^{-2}}$, cells short-circuit regardless of the electrolyte used after only about 100 cycles. Interestingly, these failures can only be detected in the voltage profiles by the

absence of the previously mentioned stripping artefacts, close to the upper cut-off voltage.

Without the correlation to coulombic efficiency, cells appear to behave similarly to symmetric cells (overview in Figure S10, enlarged depiction in Figure S11), instead of exhibiting rectangular voltage profiles that would normally be expected for irreversibly short-circuited cells. This could be an indication for the occurrence of soft short-circuits and not complete cell failure, but "pretending" symmetric cell behaviour and continuing to cycle at reduced overpotential.

When now keeping the amount of cycled lithium metal at a constant thickness of 10 μm (Figures S12 and S13), once again similarities to symmetric cells can be seen. A remarkable difference, however, can be noticed for the duration of lithium stripping, easiest to see when looking at the cells cycled at $0.1 \, \mathrm{mA \cdot cm^{-2}}$ for 20 h: the plating step (lithium is removed from the Li electrode and plated onto the Cu substrate) always takes the pre-set time. The reverse process, the stripping of the metal from the copper surface, however, concludes much earlier, especially in the case of the carbonate electrolyte. This again gives a hint that cycling of the lithium metal is not as efficient as previously assumed in symmetric cell tests.[43,46]

Figure S13 provides more information about the cycling efficiency at different speeds. In general, cycling over the first twenty cycles (see also Figure S14) is relatively efficient, with coulombic efficiencies usually over 90%. After that, strong differences between the two electrolytes can be seen. At medium current densities (Figure S13b and c), the efficiency of carbonate electrolyte cycling declines significantly, with a tendency to short-circuit towards the end of cycling. The ether electrolyte exhibits better behaviour: while it also shows slight instabilities (Figure S13c), overall coulombic efficiency remains high. Only at the highest cycling speed (Figure S13d), both

Batteries & Supercaps

Articles
doi.org/10.1002/batt.202100145

Chemistry Europe
European Chemical
Societies Publishing

electrolytes fail after around 100–200 cycles, but also here the carbonate exhibits poorer performance before the cell failure.

Generally, the results with asymmetric cells already show how important choosing the right model system is. Many of the effects seen in this part of the study were not well visible with Li||Li cells. Only by introducing a copper electrode and thus removing a lithium repository on one of the two sides of the cell it is possible to see how inefficient lithium metal cycling in the given electrolytes actually is.

2.2.2. Influence of Electrolyte Volume

As the difference between symmetric and asymmetric cells was so significant, the influence of reduced electrolyte volume was also investigated in the Cu||Li configuration. These results can be found in Figures S15–S18, where both voltage profiles and coulombic efficiencies are shown. As with the experiments carried out before, it can be seen that cell stability is again significantly lower than with comparable symmetric cells (Figures S5–S8). In general, very little information can be extracted from the polarization profile development, especially at higher current density, as these are quite noisy. CE, however, provides valuable insights. At a low current density of $0.1 \, mA \cdot cm^{-2}$ (Figure S16a), cells survive for the full 500 cycles regardless of the quantity of electrolyte, however a slightly lower CE is recorded for the carbonate electrolyte at the lowest volume of 50 µL. When current is increased to $0.5 \, mA \cdot cm^{-2}$ (Figure S16b), first instabilities can be seen with the carbonate electrolyte, though in general cycling is still relatively stable. At the two highest current densities (Figure S17), it becomes clear that cells survive only for a very limited time regardless of the electrolyte. While at $1.0 \, mA \cdot cm^{-2}$, cycling with the ether electrolyte works above an electrolyte volume of 100 µL – the

carbonate exhibits generally poor performance, and at $2.0 \, mA \cdot cm^{-2}$ satisfactory results cannot be achieved for any electrolyte quantity. Even with 500 µL, cells only cycle for a short period of around 100 cycles before short-circuits start to dominate.

An interesting difference to symmetric cell tests is that a drying-out of the electrolyte, indicated by steeply rising polarization, does not appear in asymmetric cells at the electrolyte volumes tested, even with the lowest repository of electrolyte present in the cell. This indicates a substantial contribution of the metallic lithium anode to electrolyte degradation, which is already minimised in asymmetric cells. The low amount of lithium plated onto the copper substrate does not contribute to drying out of the cell as much as a bare lithium anode does.

2.2.3. Influence of Edge Protection

An important factor promoting the formation of dendrites are locally high current densities. While in a model system a uniform current density across the electrode surface is usually assumed, in reality, surface roughness and, especially, electrode edges play a significant role.[47–49] This led to the working hypothesis that a fair share of the soft short-circuits observed in the experiments presented so far could have originated from the dendrite growth at electrode edges. To further examine this effect, asymmetric cells with and without a HDPE gasket, insulating the lithium metal edges, were cycled at $1.0 \, mA \cdot cm^{-2}$, with a step time of 1 h per plating/stripping step (corresponding to 5 µm of Li), a set of experimental parameters that already showed to be critical for cell failure.

The direct comparison of unprotected (red) and insulating-gasket-protected cells (blue) can be seen for both electrolytes in Figure 5. At first sight, the profiles look very similar to each
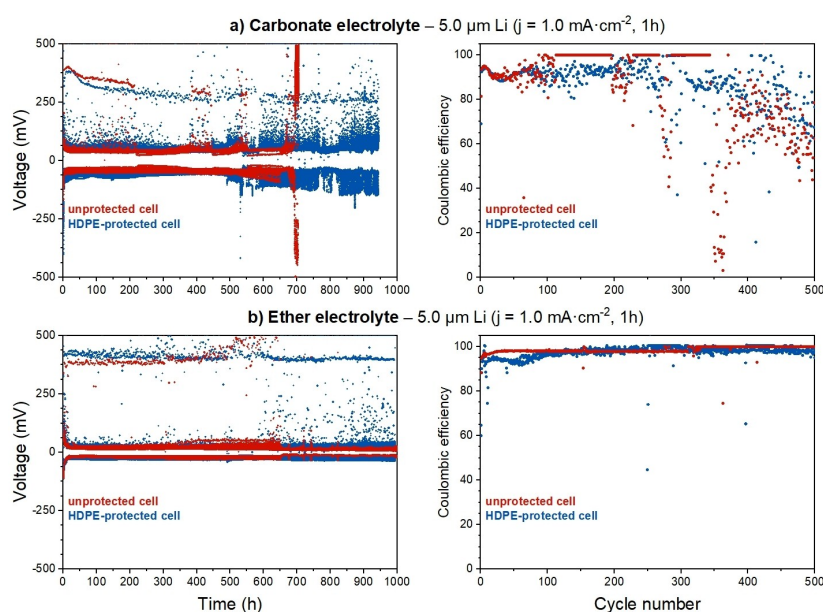

Figure 5. Polarization development and coulombic efficiency of the unprotected and protected asymmetric (Cu||Li) cells.

Batteries & Supercaps

Articles
doi.org/10.1002/batt.202100145

Chemistry
Europe
European Chemical
Societies Publishing

other, especially in the beginning, with the HDPE-protected cells exhibiting just a slightly higher overpotential. Only after prolonged cycling, it can be seen that the unprotected, carbonate electrolyte-filled cell short-circuits after about 700 hours. At a similar time, for the unprotected ether electrolyte cell the overpotential drops slightly. The protected cells, in contrast, show no complete cell failures for both electrolyte types. The coulombic efficiency data exhibit notable differences between protected and unprotected electrodes in case of carbonate electrolyte. When no protection was used, soft short-circuits for the carbonate electrolyte cell already occurred after about 100 cycles. These were partially reversible, but overall, a poor performance can be seen, while with edge-protection, these soft shorts are avoided. The efficiency, though not always stable with the carbonate, remains at around 80%–90% for the first 300 cycles, after which it drops down to about 50% towards the end of the measurement. In contrast, the ether electrolyte-filled cells show negligible difference between protected and unprotected edge configurations.

However, when taking a closer look, it becomes clear that after about 300 cycles, the unprotected cell has a coulombic efficiency of exactly 100%, indicating a short-circuit. This shows that protection helps to suppress dendrites originating from electrode edges, and thus have a positive effect for cycling efficiency, as well. To sum up, the deceptive nature of the results, obtained with symmetric cells, relying purely on the voltage profile (overpotential growth) can be underlined. Moreover, there is a hint for electrode edges playing a role in the development of short-circuits within the cell. Protecting edges seems to give a clearer image of the real coulombic efficiency of lithium plating and stripping and can help to validate the feasibility of remedies for alleviating the shortcomings of lithium metal. It is especially important in small research cells with large electrode edge length to electrode area ratio; as most of the research grade cells are often used in flooded configuration, promoting lithium edge activity. However, even in large cells with lean electrolyte the dominance of edge-promoted short circuits is expected.

2.3. Reversibility of Li Cycling

Cycling a pre-set amount (thickness, in case of identical area of electrode is used) of lithium always raises a question, what actual thickness of lithium is deposited and can be reversibly removed. Quantifying the reversible lithium deposition and stripping gives one more tool to assess the efficiency of the lithium cell cycling. *Operando* measurements in this direction have been done previously, for example using holographic interferometry[50] or setups with a pressure sensor.[51] However, the focus there was on the thickness development of an electrode over prolonged cycling. For this reason, we chose to employ a more sensitive technique – nano-dilatometry – that has also been successfully used for tracking the expansion and shrinkage of various LIB anodes and cathodes *operando* previously.[52–58] While dilatometry measurements on metallic lithium and copper electrodes have not been reported yet, it

seems to be an ideal tool for the purpose. Dilatometry would allow us to track the build-up of deposited lithium very closely throughout the entire measurement. Compared to coin-cell type experiments, a major advantage of this setup is that the thickness of a selected electrode could be tracked throughout the entire measurement. Monitoring electrode thickness helps to gain further insights into the plating and stripping behaviour of metallic lithium, especially when a comparative study with protected and unprotected electrode edges is carried out. Irreversible and reversible parts of the lithium cycling can be separated in post-processing by doing a simple baseline calculation. Analogous to previous experiments, cells were cycled at a maximum current density of $2.0 \ mA \cdot cm^{-2}$, by default using working electrodes with a diameter of 7.5 mm. At this size, all electrode edges are directly exposed to the electrolyte. In a second step, all experiments were performed with 10 mm diameter electrodes at the same current density, this time making sure that all edges were protected by the polyether ether ketone (PEEK) encapsulation of the cell. Under these conditions, dendrite growth on the edges is expected to be mechanically suppressed.

2.3.1. Thickness Changes of Li Deposits on Metallic Lithium Electrodes

The behaviour of lithium electrodes was examined with the both aforementioned electrolyte types, to study the electrolyte-dependent deposition and stripping efficiency, Figure 6. In case, where a smaller lithium electrode is used with exposed edges, it allowed studying the contribution of edge effects to the results of cycling on the one hand, and on the thickness change of the electrode, on the other.

A remarkable feature of both tests is the overall thickness reduction (!) of the lithium electrode, especially in the beginning of the experiment, as such a shrinkage would be expected for stripping (or de-intercalation) of the cell,[56] but not during deposition of metallic lithium on the surface. Over the first five hours, the electrode thickness decreased by over 10 μm regardless of the electrolyte. In the case of the ether electrolyte (Figure 6b), this decrease is stagnating towards the end of the experiment, with tiny reversible peaks being visible towards the end of each plating step. There is no irreversible growth that would lead to an increase of metal thickness, unlike in the case of the carbonate, where, after initial shrinkage for the first two cycles, the electrode increases in thickness again. Interestingly, reversible peaks cannot only be observed for plating steps, but also – though to a more limited degree – during stripping, pointing at some kind of realignment of metallic lithium under electrochemical stripping conditions. Keeping in mind that we theoretically move 10 μm of lithium in each half-cycle (according to a current applied), the shrinkage of the electrode thickness is rather surprising, pointing towards preferential plating of metal on the electrode edges. The empty space between the lithium electrode and the electrode holder promotes most of lithium being plated on the lithium electrode edge, while stripping, in the beginning for
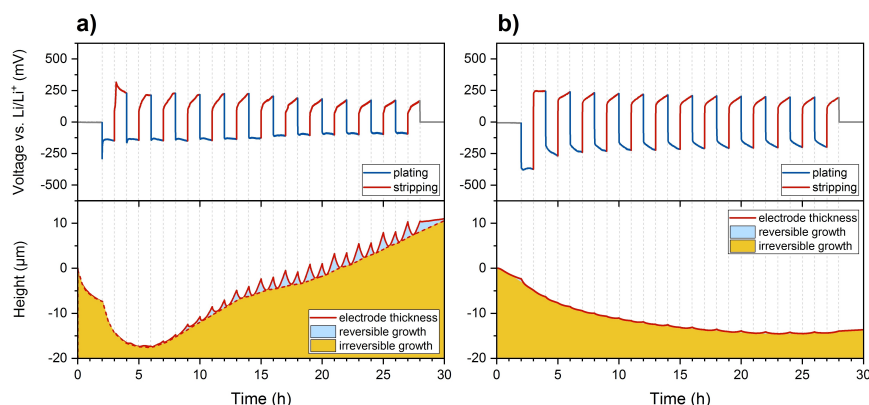
Batteries & Supercaps

Articles
doi.org/10.1002/batt.202100145

Chemistry Europe
European Chemical
Societies Publishing

Figure 6. Li||Li dilatometry cell with the electrode edges exposed to the electrolyte: a) the carbonate and b) the ether electrolyte; at 2.0 mA·cm^{-2} for 12 cycles.

both electrolytes and later at least in the case of ether electrolyte, preferentially from the plane of lithium disc. The tendency for lithium deposition on edges was confirmed after the disassembly of the cell, where dull grey deposits could mainly be observed at the electrode edge and less on the electrode surface (Figure S19).

Next, we tested protected lithium electrodes under the same experimental conditions (Figure 7). The most notable difference to the previous tests is the change of direction in electrode thickness. Unlike before, no shrinkage can be seen, instead, in both electrolytes irreversible growth dominates, yet to a different extent. In the ether electrolyte, irreversible growth remains below 15 μm, with clear reversible peaks appearing during plating. By contrast, the irreversibility in the case of the carbonate electrolyte is increased steeply almost by a factor of ten during the first 5–7 h, and then plateaus at the thickness of about 130 μm. It can be suspected that the origin of this massive initial growth lies not in the irreversible lithium metal cycling but due to the decomposition of electrolyte and the thick SEI formation, which explains as well barely visible reversible peaks upon lithium plating. In addition, we are using highly fluorinated electrolyte (containing 20% of FEC), which is prone to formation of LiF spheres,[59] with their size depending

on the local environment in the cell, such as active materials and conducting salt. Reversible peaks can be observed during the plating steps, however, the previously observed maxima during stripping steps have disappeared altogether. This further supports the hypothesis that they have originated from a realignment of metal from the electrode edge to the surface.

Still, the total thickness difference between plated and stripped state of electrode does not account for the theoretically expected 10 μm. It can be assumed that these effects would be much better seen on a different substrate. In the case of a metallic lithium electrode, two main effects come into play when looking at the thickness difference. Firstly, lithium stripping does not necessarily take place from the area where metal has been deposited, but where it is 'easiest', that is, energetically most favourable. During the stripping, therefore, it is expected that metal be removed from the bulk lithium metal instead of the deposited material (a similar process as pitting corrosion).

However, when comparing protected and unprotected lithium metal electrodes, a notable difference between the testing outcomes can be seen clearly. When there is space for lithium deposition in other places than the electrode surface, results might be false.
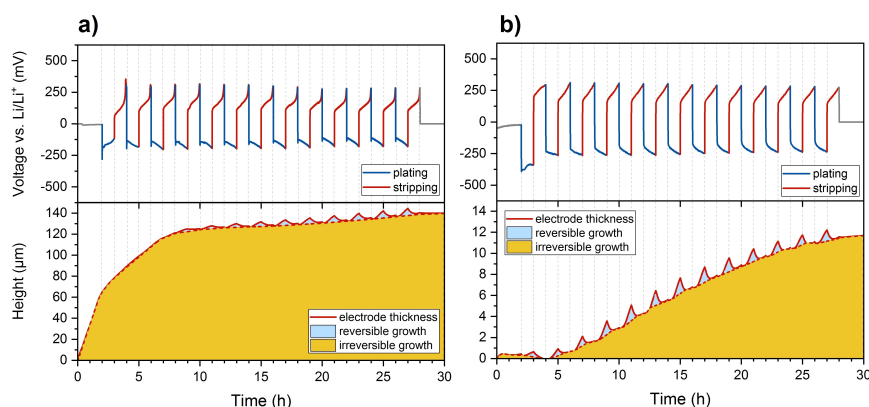

Figure 7. Li||Li dilatometry cell with covered electrode edges. Electrolytes used were a) the carbonate and b) the ether electrolyte; cycling took place at 2.0 mA·cm^{-2} for 12 cycles. Please note the different scaling of the height.

2.3.2. Thickness Changes of Li Deposits on Copper Current Collector

The same experimental setup was used for monitoring lithium deposition onto and stripping from copper current-collector, using both a smaller diameter, with edges exposed to electrolyte (Figure 8) and larger diameter copper disc with mechanically protected edges (Figure 9).

Unsurprisingly, unlike for metallic lithium electrode, no shrinkage of the electrode can be observed in case of unprotected edges, as only growth of lithium deposits is possible. A main difference to the measurements carried out with lithium electrodes is the much shorter duration of each cycle, originating from significantly shortened stripping steps. This indicates that the stripping of lithium metal from the copper surface is, compared to plating, highly inefficient, and some electrochemically inactive lithium remains on the electrode surface. While the irreversible growth is limited for the ether electrolyte, again a massive increase of the electrode thickness can be seen for the carbonate one. For the latter, the stripping steps are significantly shorter than the plating ones, indicating that the reduction of electrolyte (most likely dominated by FEC) is a preferential reaction taking place during

cycling of the battery. In general, carbonate electrolytes with $LiPF_6$ salt are known to exhibit poor cycling efficiency on copper substrate,[60] which in this case might be even further amplified by the reduction of electrolyte (especially the FEC), which is a preferential reaction taking place during cycling of the battery. However, for both electrolyte types, a reversible thickness change can be seen, which is peaking when the lithium plating is complete. The difference between plated and stripped state is again below the theoretically possible 10 μm, pointing at suboptimal deposition of lithium when edges are exposed to the electrolyte.

Significant differences can be seen when the copper electrode is of the larger size, making the edges of copper current collector inaccessible to the electrolyte (Figure 9).

It can be observed that reversible growth is pronounced for both electrolytes, with the thickness change coming extremely close to the theoretically expected value of around 10 μm of deposited metal. Clear, sharp maxima in both cases show efficient plating and stripping of the lithium on the copper substrates. When looking at the irreversible growth processes, again a low increase can be noticed for the ether electrolyte (around 10 μm in total at the end of cycling), while the carbonate electrolyte leads a massive build-up of irreversible
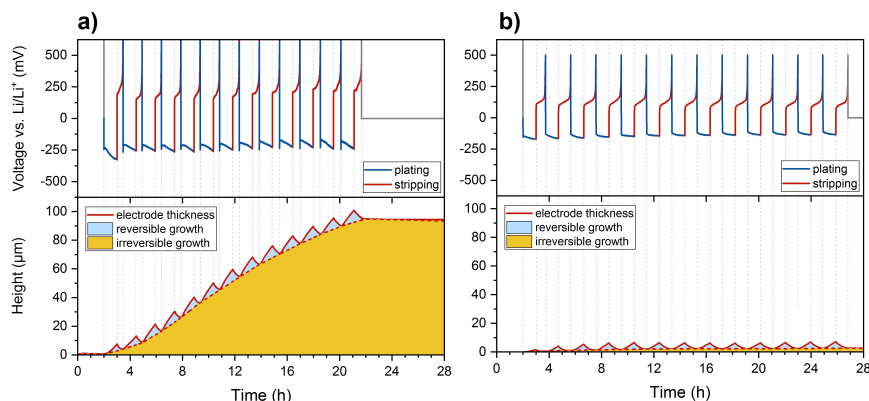

Figure 8. Cu∣∣Li dilatometry cell with the electrode edges exposed to the electrolyte. Electrolytes used were a) the carbonate and b) the ether electrolyte; cycling took place at 2.0 mA·cm^{-2} for 12 cycles.
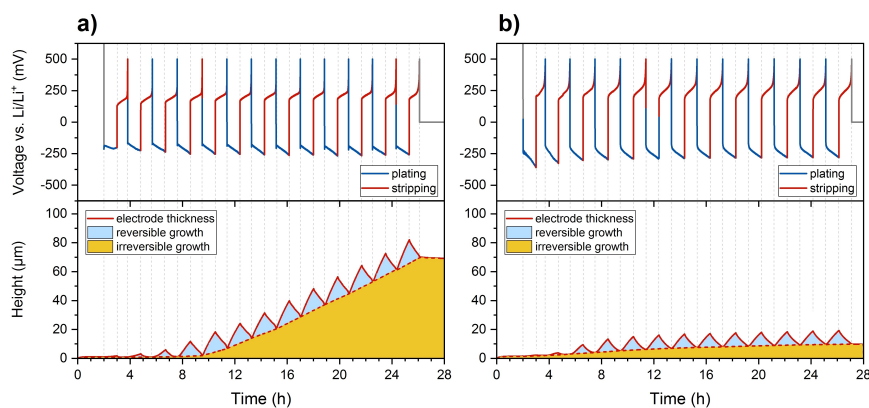

Figure 9. Cu∣∣Li dilatometry cell with covered electrode edges. Electrolytes used were a) the carbonate and b) the ether electrolyte; cycling took place at 2.0 mA·cm^{-2} for 12 cycles.

Batteries & Supercaps

Articles
doi.org/10.1002/batt.202100145

Chemistry Europe
European Chemical
Societies Publishing

growth (final irreversible thickness 70 μm). Once again, this points at formation of decomposition products, namely LiF spheres, in the FEC-containing carbonate electrolyte.

When now comparing the results to the previous experiments with unprotected copper electrodes, two main differences can be observed: firstly, the duration of lithium stripping is greatly increased for the carbonate electrolyte, indicating improved efficiency of lithium cycling with edge protection. This also is reflected in the increased duration of the experiment, which went up from 22 hours (unprotected Cu) to 26 hours (protected) for 12 full cycles. In addition, a decrease of irreversible growth by around 40% compared to the unprotected electrode can also be noticed for the carbonate electrolyte. While for the ether electrolyte, no such decrease can be seen (performance with the unprotected electrode was already acceptable), reversible peaks are also much more pronounced in the protected setup and come very close to the theoretical value of 10 μm. The second main difference with protected electrodes is the increased polarization of the cells. This higher overpotential can be ascribed to the fact that preferred locations for lithium deposition and removal were deliberately blocked by the edge protection, and thus a higher electrochemical barrier has to be overcome for cycling of the cell.

Finally, when comparing the results with copper electrodes with the previous lithium electrode experiments, it becomes clear that edge protection is a non-negligible factor. Especially when using copper electrodes, as is common in asymmetric Cu||Li and 'anode-free' cell layouts, edge protection is crucial for obtaining high cycling efficiency and enabling reversible lithium plating while minimising side reactions, as became especially apparent for the carbonate electrolyte. For lithium metal electrodes, the most significant effect seen in these short-term experiments was the massive reduction of electrode thickness in the first few cycles (pointing at preferential edge deposition), however, the impact on cycling behaviour and efficiency was minimal. Nevertheless, as side reactions are mitigated by the application of edge protection, there might be a beneficial effect on the lifespan of lithium metal electrodes, as well. In general, it remains to be seen whether restricting Li metal cycling to the electrode surface also leads to an increased formation of needle dendrites, though studies suggest needle-like deposition is most favoured in areas with locally increased current density. The deposition of metal on flat surfaces with uniform current density should be dominated by mossy morphology.[61]

3. Conclusions

The impact of different experimental factors on the performance of lithium metal batteries have been evaluated in this study. Symmetric cells, as an ideal model system to verify characterization flaws, were investigated in comparison to asymmetric cells with bare copper as a counter electrode and a base for lithium plating. Among the experimental parameters, effects of electrolyte type and its amount, current density and the total charge amount (that is, amount of lithium) were investigated.

With both cell types, clear trends and a good experimental reproducibility were obtained. However, we could identify the deceptive nature of tests in symmetric cells and with a large excess of electrolyte, as both can massively cover up degradation effects in a cell. Especially at elevated current densities around 1.0 mA·cm^{-2}, results became much more variable, as cells appeared to cycle normally, but were operating at drastically decreasing efficiency, as tests with asymmetric configuration confirmed.

In addition, the contribution of electrode edges was qualitatively investigated by introducing a new cell configuration with protected electrode edges. By the addition of edge protection only allowing plating and stripping on the electrode plane, cycling efficiencies and cell lifetimes were greatly improved, however, at the cost of increased overpotentials. This became especially apparent in operando dilatometry studies, where cells without such protection were giving nonsensical result, such as decrease in electrode thickness upon plating, due to preferential deposition of dendritic lithium on the electrode edges. These effects – namely low cycling reversibility and unexpected shrinkage of lithium electrodes – were greatly alleviated by switching to electrodes with protection.

3.1. Recommendations

For future studies on enabling metallic lithium as an anode, accounting for these pitfalls should form an integral part of experimental design. Stable and reproducible long-term cycling under recommended conditions would give a better indication for improved performance than low current, low capacity experiments with excess of lithium and electrolyte. We therefore recommend implementing the following measures:

a) *Cell setup:* Limit the presence of excess metal that could cover up cell degradation – thin lithium foils (thickness < 50 μm) in asymmetric cell configuration should be preferred.

b) *Electrolyte:* A large excess of electrolyte should be avoided to clearly see the full extent of degradation. Quantities of less than 100 μL·cm^{-2} of electrolyte should be used in laboratory cells with a large dead volume, while in standard coin cells or pouch-type cells the amount should not exceed 20 μL·cm^{-2}.

c) *Current densities:* The current densities of magnitude, corresponding to the ones to be applied in intended application, should be used. A critical minimum current density of 1.0 mA·cm^{-2} or above should be selected.

d) *Capacity (amount of lithium):* Similarly, capacities at least above 1.0 mAh·cm^{-2} (better 2–3 mAh·cm^{-2}) would be most relevant for practical use.

e) *Edge protection:* Preferential plating and stripping of dendritic Li can take place on electrode edges. To avoid erroneous results due to unwanted negative volume

Batteries & Supercaps

Articles
doi.org/10.1002/batt.202100145

Chemistry Europe
European Chemical
Societies Publishing

changes of the electrode and formation of dendritic pathways on edges, these should be protected.

Experimental Section

Cell assembly & cycling

Cells were assembled in an argon-filled glove box (O_2 and H_2O concentration below 0.1 ppm) using a in-house-engineered coin-cell-type[62] two-electrode setup. The symmetric cells consisted of two identical, circular lithium discs with a diameter of 13 mm. For asymmetric cells, a Copper foil of identical diameter replaced the Li disc on the working electrode side. Commercial polypropylene separator foil (CG2400, Celgard LLC, USA) with a diameter of 17 mm was used as a separator. After the desired amount of electrolyte was added to the cells, they were closed with a torque wrench, ensuring constant stack pressure. Cells were galvanostatically tested in duplicates on an Astrol battery cycler (Astrol Electronic AG, Switzerland) and a constant temperature of 25 °C. Current densities were in a range from 0.1 to 2.0 mA cm^{-2} with cut-off potential limits set to ±500 mV vs. Li/Li$^+$. Cycling commenced after 2 h of open-circuit potential.

Dilatometry measurements

In addition to standard cell experiments, the thickness change of symmetric and asymmetric cells during cycling was monitored in a commercial three-electrode dilatometry cell setup (ECD-3, EL-Cell, Germany).[58] The same electrode materials as for the standard cells were used. By default, the working electrode had a diameter between 7.5–10 mm, the counter electrode a diameter of 12 mm. In addition, the setup also contained a third Li reference electrode (diameter 1 mm). A porous glass T-frit dried at 120 °C overnight served as a separator. All components were placed together in a polyether ether ketone (PEEK) encapsulation in the cell body, and the cells then filled with 500 μL (corresponding to 636 μL·cm^{-2} with respect to electrode area) of electrolyte. The same electrolytes as for standard cells were used. After the cell was sealed with a stainless steel membrane, a pressure sensor was applied on top of the cell stack to measure thickness changes during the experiment. After a two-hour resting period at open-circuit potential, cells were galvanostatically cycled for 12 cycles at a current density of 2.0 mA·cm^{-2} on a BioLogic SP-150 (Bio-Logic Science Instruments, France) potentiostat for one hour per plating and stripping step. The same cut-off potential limits as for standard cells was set. Thickness data were recorded continuously from the beginning of the relaxation period until 2 hours after the end of cycling to monitor any delayed thickness changes.

Materials

Lithium electrodes were punched from pristine lithium ribbon with 0.75 mm thickness and 15 mm width (Alfa Aesar, 99.9% purity) and used without further treatment. Standard copper electrodes were punched out of 20 μm thick copper foil (Goodfellow Cambridge, 99.9% purity), thoroughly washed with absolute ethanol and dried at 120 °C in vacuum over night before introducing them to the glovebox. Further foils with higher purity grades were used for evaluating the influence of the copper composition on cycling performance: high-purity copper foil with a thickness of 20 μm (Goodfellow Cambridge, >99.99% purity) and both annealed and hard oxygen-free high-conductivity copper foil with a thickness of 25 μm (Goodfellow Cambridge, >99.95% purity). The preparation procedure was identical to the standard foil.

Electrolytes

The experiments were carried out with two types of electrolyte, one carbonate- and one ether-based. A 20:80 (v/v) mixture of FEC (BASF) and DMC (Gotion) with 1 M LiPF$_6$ (Sigma Aldrich) was used as the carbonate electrolyte, while a 2:1 (v/v) mixture of DME and DOL with 1 M LiTFSI (Gotion) with a 0.5 M LiNO$_3$ additive (Sigma Aldrich) was used as the ether electrolyte. By default, 500 μL (380 μL·cm^{-2} with respect to electrode area) of electrolyte were applied to the separator material of the cell. Before inserting the counter electrode and sealing the cell, it was made sure that the separator was well wetted with electrolyte. For certain experiments, lower quantities of 250 μL (190 μL·cm^{-2}), 100 μL (76 μL·cm^{-2}) and 50 μL (38 μL·cm^{-2}) electrolyte were used.

Edge protection

For some cells the outer edges of the lithium metal electrode were protected with insulating material. In standard cell experiments, HDPE foil with 2 μm thickness (Goodfellow Cambridge) was cut into rings with 15 mm outer and 7.5 mm inner diameter and placed between metal surface and separator to cover the metal edges. The current density in the experiments was adjusted accordingly to the smaller electrode area exposed to separator and electrolyte. To provide for electrode edge protection in the dilatometry cell, the diameter of the working electrode was increased from the standard 7.5 mm to the inner diameter of the PEEK insulation (10 mm).

Conflict of Interest

The authors declare no conflict of interest.

[1] H. F. Bauman, J. E. Chilton, W. J. Conner, G. M. Cook, *New Cathode-Anode Couples Using Nonaqueous Electrolyte*, Sunnyvale CA **1963**.
[2] H. Shimotake, G. L. Rogers, E. J. Cairns, *Ind. Eng. Chem. Process Des. Dev.* **1969**, *8*, 51–56.
[3] H. F. Bauman, *Limited-Cycle Secondary Battery Using Lithium Anode*, US Air Force Report APL-TDR-64-59, **1964**.
[4] R. Jasinski, *Electrochem. Technol.* **1968**, *6*, 28–35.
[5] R. G. Selim, K. R. Hill, B. M. L. Rao, *Research and Development of a High Capacity, Nonaqueous Secondary Battery*, NASA Report CR-54969, **1965**.
[6] J. O. Besenhard, G. Eichinger, *J. Electroanal. Chem. Interfacial Electrochem.* **1976**, *68*, 1–18.
[7] K. M. Abraham, *J. Power Sources* **1985**, *14*, 179–191.
[8] K. Kanehori, K. Matsumoto, K. Miyauchi, T. Kudo, *Solid State Ionics* **1983**, *9–10*, 1445–1448.
[9] M. Uchiyama, S. Slane, E. Plichta, M. Salomon, *J. Power Sources* **1987**, *20*, 279–286.
[10] A. Yoshino, K. Sanechika, T. Nakajima, *Secondary Battery* **1986**, US4668595 A.
[11] S. Megahed, B. Scrosati, *J. Power Sources* **1994**, *51*, 79–104.
[12] R. Wang, W. Cui, F. Chu, F. Wu, *J. Energy Chem.* **2020**, *48*, 145–159.

Batteries & Supercaps

Articles
doi.org/10.1002/batt.202100145

Chemistry
Europe
European Chemical
Societies Publishing

[13] A. Varzi, K. Thanner, R. Scipioni, D. Di Lecce, J. Hassoun, S. Dörfler, H. Altheus, S. Kaskel, C. Prehal, S. A. Freunberger, *J. Power Sources* **2020**, *480*, 228803.

[14] E. J. Berg, C. Villevieille, D. Streich, S. Trabesinger, P. Novák, *J. Electrochem. Soc.* **2015**, *162*, A2468–A2475.

[15] S. Urbonaite, T. Poux, P. Novák, *Adv. Energy Mater.* **2015**, *5*, 1500118.

[16] S. Urbonaite, P. Novák, *J. Power Sources* **2014**, *249*, 497–502.

[17] X.-Q. Zhang, X.-B. Cheng, X. Chen, C. Yan, Q. Zhang, *Adv. Funct. Mater.* **2017**, *27*, 1605989.

[18] J. Xiang, Y. Zhao, L. Yuan, C. Chen, Y. Shen, F. Hu, Z. Hao, J. Liu, B. Xu, Y. Huang, *Nano Energy* **2017**, *42*, 262–268.

[19] X.-T. Xi, X. Feng, X.-J. Nie, B.-H. Hou, W.-H. Li, X. Yang, A.-B. Yang, W.-D. Sun, X.-L. Wu, *Chem. Commun.* **2019**, *1*, DOI 10.1039/C9CC03175H.

[20] X.-B. Cheng, T.-Z. Hou, R. Zhang, H.-J. Peng, C.-Z. Zhao, J.-Q. Huang, Q. Zhang, *Adv. Mater.* **2016**, *28*, 2888–2895.

[21] R. Miao, J. Yang, Z. Xu, J. Wang, Y. Nuli, L. Sun, *Sci. Rep.* **2016**, *6*, 2–10.

[22] F. Ding, W. Xu, G. L. Graff, J. Zhang, M. L. Sushko, X. Chen, Y. Shao, M. H. Engelhard, Z. Nie, J. Xiao, X. Liu, P. V. Sushko, J. Liu, J. G. Zhang, *J. Am. Chem. Soc.* **2013**, *135*, 4450–4456.

[23] K. N. Wood, M. Noked, N. P. Dasgupta, *ACS Energy Lett.* **2017**, *2*, 664–672.

[24] Q. Li, S. Tan, L. Li, Y. Lu, Y. He, *Sci. Adv.* **2017**, *3*, 1–10.

[25] G. Yasin, M. Arif, T. Mehtab, X. Lu, D. Yu, N. Muhammad, M. T. Nazir, H. Song, *Energy Storage Mater.* **2019**, *25*, 644–678, DOI 10.1016/j.ensm.2019.09.020.

[26] N. Gao, A. W. Abboud, G. S. Mattei, Z. Li, A. A. Corrao, C. Fang, B. Liaw, Y. S. Meng, P. G. Khalifah, E. J. Dufek, B. Li, *Small Methods* **2021**, *5*, 2000807.

[27] C. Fang, X. Wang, Y. S. Meng, *Trends Chem.* **2019**, *1*, 152–158.

[28] B. Liu, J. G. Zhang, W. Xu, *Joule* **2018**, *2*, 833–845.

[29] J. Liu, Z. Bao, Y. Cui, E. J. Dufek, J. B. Goodenough, P. Khalifah, Q. Li, B. Y. Liaw, P. Liu, A. Manthiram, Y. S. Meng, V. R. Subramanian, M. F. Toney, V. V. Viswanathan, M. S. Whittingham, J. Xiao, W. Xu, J. Yang, X.-Q. Yang, J.-G. Zhang, *Nat. Energy* **2019**, *4*, 180–186.

[30] O. Lavi, S. Luski, N. Shpigel, C. Menachem, Z. Pomerantz, Y. Elias, D. Aurbach, *ACS Appl. Energ. Mater.* **2020**, *3*, 7485–7499.

[31] Y. Liu, X. Xu, M. Sadd, O. O. Kapitanova, V. A. Krivchenko, J. Ban, J. Wang, X. Jiao, Z. Song, J. Song, S. Xiong, A. Matic, *Adv. Sci.* **2021**, *8*, 2003301.

[32] D. Lu, Y. Shao, T. Lozano, W. D. Bennett, G. L. Graff, B. Polzin, J. Zhang, M. H. Engelhard, N. T. Saenz, W. A. Henderson, P. Bhattacharya, J. Liu, J. Xiao, *Adv. Energy Mater.* **2015**, *5*, 1400993.

[33] X.-B. Cheng, R. Zhang, C.-Z. Zhao, Q. Zhang, *Chem. Rev.* **2017**, *117*, 10403–10473.

[34] D. Aurbach, E. Zinigrad, H. Teller, P. Dan, *J. Electrochem. Soc.* **2000**, *147*, 1274.

[35] S. Jiao, J. Zheng, Q. Li, X. Li, M. H. Engelhard, R. Cao, J.-G. Zhang, W. Xu, *Joule* **2018**, *2*, 110–124.

[36] H. Yang, C. Guo, A. Naveed, J. Lei, J. Yang, Y. Nuli, J. Wang, *Energy Storage Mater.* **2018**, *14*, 199–221.

[37] D. Lu, Y. Shao, T. Lozano, W. D. Bennett, G. L. Graff, B. Polzin, J. Zhang, M. H. Engelhard, N. T. Saenz, W. A. Henderson, P. Bhattacharya, J. Liu, J. Xiao, *Adv. Energy Mater.* **2015**, *5*, 1400993.

[38] P. Albertus, S. Babinec, S. Litzelman, A. Newman, *Nat. Energy* **2018**, *3*, 16–21.

[39] A. J. Louli, M. Coon, M. Genovese, J. DeGooyer, A. Eldesoky, J. R. Dahn, *J. Electrochem. Soc.* **2021**, *168*, 020515.

[40] J. Zheng, P. Yan, D. Mei, M. H. Engelhard, S. S. Cartmell, B. J. Polzin, C. Wang, J. Zhang, W. Xu, *Adv. Energy Mater.* **2016**, *6*, 1502151.

[41] K. N. Wood, E. Kazyak, A. F. Chadwick, K.-H. Chen, J.-G. Zhang, K. Thornton, N. P. Dasgupta, *ACS Cent. Sci.* **2016**, *2*, 790–801.

[42] K.-H. Chen, K. N. Wood, E. Kazyak, W. S. LePage, A. L. Davis, A. J. Sanchez, N. P. Dasgupta, *J. Mater. Chem. A* **2017**, *5*, 11671–11681.

[43] J. Xiao, Q. Li, Y. Bi, M. Cai, B. Dunn, T. Glossmann, J. Liu, T. Osaka, R. Sugiura, B. Wu, J. Yang, J.-G. Zhang, M. S. Whittingham, *Nat. Energy* **2020**, *5*, 561–568 .

[44] F. J. Günter, C. Burgstaller, F. Konwitschny, G. Reinhart, *J. Electrochem. Soc.* **2019**, *166*, A1709–A1714.

[45] H. Li, D. Chao, B. Chen, X. Chen, C. Chuah, Y. Tang, Y. Jiao, M. Jaroniec, S.-Z. Qiao, *J. Am. Chem. Soc.* **2020**, *142*, 2012–2022.

[46] B. D. Adams, J. Zheng, X. Ren, W. Xu, J.-G. Zhang, *Adv. Energy Mater.* **2018**, *8*, 1702097.

[47] H. Lee, S. Chen, X. Ren, A. Martinez, V. Shutthanandan, M. Vijayakumar, K. S. Han, Q. Li, J. Liu, W. Xu, J.-G. Zhang, *ChemSusChem* **2018**, *11*, 3821–3828.

[48] C. A. Calderón, A. Vizintin, J. Bobnar, D. E. Barraco, E. P. M. Leiva, A. Visintin, S. Fantini, F. Fischer, R. Dominko, *ACS Appl. Energ. Mater.* **2020**, *3*, 2020–2027.

[49] J. Bobnar, A. Vizintin, G. Kapun, C. Njel, R. Dedryvère, R. Dominko, B. Genorio, *Batteries and Supercaps* **2021**, *4*, 623–631.

[50] M. Ota, S. Izuo, K. Nishikawa, Y. Fukunaka, E. Kusaka, R. Ishii, J. Selman, *J. Electroanal. Chem.* **2003**, *559*, 175–183.

[51] S. Sheng, L. Sheng, L. Wang, N. Piao, X. He, *J. Power Sources* **2020**, *476*, 228749.

[52] J. L. Gómez-Cámer, C. Bünzli, M. M. Hantel, T. Poux, P. Novák, *Carbon* **2016**, *105*, 42–51.

[53] M. Winter, G. H. Wrodnigg, J. O. Besenhard, W. Biberacher, P. Novák, *J. Electrochem. Soc.* **2000**, *147*, 2427.

[54] D. Sauerteig, S. Ivanov, H. Reinshagen, A. Bund, *J. Power Sources* **2017**, *342*, 939–946.

[55] M. Li, Z. Wang, E. Detsi, *J. Electrochem. Soc.* **2020**, *167*, 050505.

[56] I. Escher, G. A. Ferrero, M. Goktas, P. Adelhelm, *Adv. Mater. Interfaces* **2021**, 2100596.

[57] H. Michael, R. Jervis, D. J. L. Brett, P. R. Shearing, *Batteries and Supercaps* **2021**, *4*, 1378–1396.

[58] H. Michael, F. Iacoviello, T. M. M. Heenan, A. Llewellyn, J. S. Weaving, R. Jervis, D. J. L. Brett, P. R. Shearing, *J. Electrochem. Soc.* **2021**, *168*, 010507.

[59] Y. Surace, D. Leanza, M. Mirolo, C. Vaz, M. El Kazzi, P. Novák, S. Trabesinger, *E-MRS 2019 Spring Meet.*, European Materials Research Society, **2019**.

[60] G. Yang, Y. Li, S. Liu, S. Zhang, Z. Wang, L. Chen, *Energy Storage Mater.* **2019**, *23*, 350–357.

[61] J.-G. Zhang, W. Xu, W. A. Henderson, *Lithium Metal Anodes and Rechargeable Lithium Metal Batteries*, Springer International Publishing, Cham **2017**.

[62] H.-J. Peng, *Unravelling the Cell Ageing Phenomena in Aprotic Lithium-Nickel-Cobalt-Manganese-Oxide Batteries*, ETH Zürich **2016**.